A Fast Multipole Boundary Integral Equation Method for Periodic Boundary Value Problems in Three Dimensional Elastostatics and its Application to Homogenisation (first draft)

Y.Otani*and N.Nishimura†

September 11, 2006

Abstract

This paper presents a Fast Multipole Method (FMM) for periodic elastostatic problems in 3D. The proposed method periodises the solution by using replica cells, but none of the lattice sums involved are divergent and, hence, there is no mathematical ambiguity in the formulation. We estimate macroscopic elastic constants of composites with rigid inclusions using the periodic FMM and the homogenisation theory which requires solutions of periodic boundary value problems for the microstructure. Good agreement is achieved between the macroscopic elastic constants obtained with the proposed method and those obtained with micromechanics.

1 Introduction

Fast Multipole Method (FMM. See Nishimura[1] for references) is now deemed to be an essential tool for solving large scale problems with Boundary Integral Equation Method (BIEM) or Boundary Element Method (BEM). Indeed, BIEM is now capable of solving problems with no less than $O(10^8)$ unknowns with the help of FMM. It is therefore considered useful in the study of composite or structured materials because their mechanical behaviour can be analysed only with large scale models. This is the more so considering recent developments of nanotechnology because new materials such as carbon nanotube based composites literally require analyses in which the smallest length scale is of the order of several nanometres. As a matter of fact, such applications of FMM have already been investigated with ordinary FMM by Liu et al.[2], for example. Even with FMM, however, it is difficult to solve problems which cover a wide range

*Department of Civil and Earth Resources Engineering, Kyoto University, Japan
†Academic Center for Computing and Media Studies, Kyoto University, Japan

of length scale. In such cases, use of multiscale analysis based on homogenisation methods is considered effective. The standard homogenisation theory uses the solution of periodic boundary value problems for the microstructure. When the microstructure is relatively simple, it may be sufficient to use standard numerical techniques such as FEM or even analytical solutions for the analysis for the microstructure. When the microstructure is complicated as in the cases of nanotechnology applications, however, the size of the microscale analysis can become quite large. It is therefore considered worth the efforts to develop FMMs for periodic boundary value problems.

As a matter of fact, FMMs for periodic problems have been investigated since the early paper by Greengard & Rokhlin[3]. Their basic idea is to put replicas of the unit cell around it periodically. However, their approach is not without mathematical ambiguity because it includes divergent series, which are replaced by finite numbers using physical arguments called 'renormalisation'. Following this work, Greengard & Helsing [4] solved two dimensional elastostatic problems using a complex variable technique. Rodin & Overfelt [5] proposed another approach for Laplace's equation in which a differentiated integral equation is used. Related investigations on periodic problems for the Stokes equation can be found in Sangani & Mo [6], Zinchenco & Davis[7] and Greengard & Kropinski[8], for example.

In this paper we shall continue these efforts in formulating FMMs for periodic problems and present an FMM for three dimensional elastostatic problems which is effective in rigid inclusion problems. One of our interests in this paper is to present a formulation in which no mathematical ambiguity exists in the process of taking lattice sums. Indeed, our approach uses absolutely convergent series only, while previous formulations often include divergent ones. The amount of computation of the proposed method is $O(N)$ in problems with N unknowns, so the complexity of the proposed approach is the same as that of the ordinary FMM.

The problem considered in this paper is an inclusion problem where an elastic matrix includes many rigid inclusions. This analysis is intended as a continuum model of carbon nanotube (CNT) based composite materials in which the axial rigidity of the inclusion (CNT) is more than 2 order of magnitude larger than that of the matrix thus allowing the use of the rigid inclusion model. The proposed method is then utilised, in conjunction with the homogenisation theory, in the evaluation of the macroscopic moduli of the fiber-reinforced materials.

As numerical examples, we show three types of problems in which the inclusions are spheres, short fibres and long fibres. Numerical solutions are validated as we compare the macroscopic elastic moduli with those obtained with Eshelby's method, self-consistent method and the Halpin-Tsai equation.

2 Formulation

2.1 Rigid body inclusion model

We first formulate the rigid body inclusion problem. See Liu et al.[2] for the motivation for introducing this model. An elastic matrix in a domain $D \in \mathbb{R}^3$ including rigid bodies is considered. The displacement u_i satisfies Navier's equation given by

$$\mu u_{i,jj} + (\lambda + \mu) u_{j,ij} = 0 \quad \text{in } D \setminus \sigma,$$

where $\sigma = \bigcup_l \sigma_{(l)}$, $\sigma_{(l)}$ stands for the domain corresponding to a piece of rigid inclusion, and the body force is assumed to be zero for the purpose of simplicity. On $\partial\sigma_{(l)}$, u_i satisfies

$$u_i = c_{(l)i} + e_{ijk} w_{(l)j} x_k \quad \text{on } \partial\sigma_{(l)}, \tag{1}$$

where $c_{(l)i}$ and $w_{(l)i}$ are constants related to the lth rigid body. Also, on each of $\partial\sigma_{(l)}$ we require the equilibrium condition given by

$$\int_{\partial\sigma_{(l)}} C_{ijkl} u_{k,l} n_j ds = 0 \quad (i = 1, 2, 3), \tag{2}$$

$$\int_{\partial\sigma_{(l)}} e_{ipq} C_{pjkl} u_{k,l} n_j y_q ds_y = 0 \quad (i = 1, 2, 3), \tag{3}$$

where n_i is the normal vector on $\partial\sigma$ directed into σ and C_{ijkl} is the elasticity tensor whose components are expressed as

$$C_{ijkl} = \lambda \delta_{ij} \delta_{kl} + \mu(\delta_{ik}\delta_{jl} + \delta_{il}\delta_{jk}).$$

The derivatives of u_i in (2) and (3) are understood to be the limits on $\partial\sigma$ from outside of σ.

In the rest of this paper we assume that the displacement field u_i extends continuously into $\sigma_{(l)}$ in the form given in (1) to be consistent with the physical interpretation that $\sigma_{(l)}$ represents a rigid body.

2.2 Homogenisation theory

We are now interested in estimating the macroscopic elastic constants of the material whose microstructure is represented by the rigid inclusion model introduced in 2.1. To this end we utilise the homogenisation theory, which we shall briefly recapitulate in this section.

We assume that the body under consideration has a periodic microstructure whose period ϵ is small compared to the macroscopic scale of the structure. As the scaled microstructure, we consider the unit cell (denoted by Y) which consists of the elastic matrix (denoted by Ω) and rigid bodies (denoted by σ) (see Figure 1). For the purpose of simplicity, we assume that σ does not intersect with the boundary of Y, although this assumption is not necessary. See **Appendix** for the required changes when σ intersects with ∂Y.

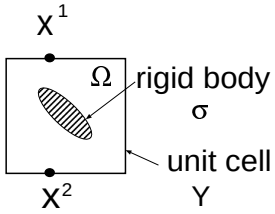

Figure 1: Unit cell

As is customary in homogenisation [9], we introduce the macroscopic and (scaled) microscopic coordinates x_i and y_i ($\sim X_i/\epsilon$, X_i: 'real' coordinate), respectively. We shall further assume that the origin O of the y coordinate system coincides with the centre of Y. With x_i and y_i the derivative with respect to the real coordinate X_i is expressed as

$$\frac{\partial}{\partial X_i} = \frac{\partial}{\partial x_i} + \frac{1}{\epsilon}\frac{\partial}{\partial y_i}. \tag{4}$$

Also, we shall use the ansatz that u_i is represented as the asymptotic expansion given by

$$u_i(X) = u_{0i}(x,y) + \epsilon u_{1i}(x,y) + \epsilon^2 u_{2i}(x,y) + \cdots \ . \tag{5}$$

The standard argument leads to

$$u_{0i}(x,y) = u_{0i}(x) \ ,$$

and

$$u_{1i}(x,y) = \frac{\partial u_{0p}}{\partial x_q}(x)\chi_i^{pq}(y), \tag{6}$$

where $\chi_i^{pq}(y)$ is a Y-periodic function to be determined. In this statement, the Y-periodicity of a function $u_i(y)$ is defined as follows: Let x^1 and x^2 be the points on the opposite sides of Y (See Figure 1). A function u_i is said to be Y-periodic if it satisfies the periodic boundary conditions given by

$$\begin{aligned} u_i(x^1) &= u_i(x^2), \\ C_{ijkl}u_{k,l}(x^1)n_j(x^1) &= -C_{ijkl}u_{k,l}(x^2)n_j(x^2), \end{aligned}$$

where the unit normal vector n_i is directed outwards from Y. The macroscopic elastic constant is then given by

$$C'_{pqrs} = \frac{1}{|Y|}\int_\Omega \left(\delta_{pi}\delta_{qj} + \chi_{i,j}^{pq}\right) C_{ijkl}\left(\delta_{rk}\delta_{sl} + \chi_{k,l}^{rs}\right) dy \tag{7}$$

once $\chi_i^{pq}(y)$ is known.

We now determine $\chi_i^{pq}(y)$. In the domain $\sigma_{(l)}$ (rigid body), (4), (5), (6) and the condition of the rigidity

$$\frac{\partial u_i}{\partial X_j} + \frac{\partial u_j}{\partial X_i} = 0$$

give

$$\chi_i^{pq}(y) = -\delta_{pi} y_q + c_{(l)i}^{pq} + e_{ijk} w_{(l)j}^{pq} y_k \quad \text{in } \sigma_{(l)} \ .$$

From the continuity of u_i throughout Y, we see that $\chi_i^{pq}(y)$ in Ω is the solution to the following periodic Dirichlet boundary value problem:

$$\mu \chi_{i,jj}^{pq} + (\lambda + \mu) \chi_{j,ij}^{pq} = 0 \qquad \text{in } \Omega, \tag{8}$$

$$\chi_i^{pq}(y) = -\delta_{pi} y_q + c_{(l)i}^{pq} + e_{ijk} w_{(l)j}^{pq} y_k \quad \text{on } \partial\sigma_{(l)}, \tag{9}$$

$$\int_{\partial\sigma_{(l)}} C_{ijkl} \chi_{k,l}^{pq} n_j ds_y = 0 \qquad \text{on } \partial\sigma_{(l)}, \tag{10}$$

$$\int_{\partial\sigma_{(l)}} e_{irs} C_{rjkl} \chi_{k,l}^{pq} n_j y_s ds_y = 0 \qquad \text{on } \partial\sigma_{(l)}, \tag{11}$$

$$\chi_i^{pq} \text{ is } Y\text{-periodic} \ , \tag{12}$$

where $c_{(l)i}^{pq}$ and $w_{(l)j}^{pq}$ are constants to be determined. We then substitute the solution χ_i^{pq} into (7) to obtain the macroscopic elastic constants C'_{ijkl} in the following form:

$$C'_{ijkl} = C_{ijkl} - \frac{1}{|Y|} \int_{\partial\sigma} t_i^{kl}(y) y_j ds, \tag{13}$$

where

$$t_i^{kl} = C_{iqrs} \chi_{r,s}^{kl} n_q + C_{iqkl} n_q.$$

2.3 FMM for periodic problems in elasticity

In this subsection, we consider the elastic periodic boundary value problem defined by (8)–(12). We shall hereafter denote the position vector corresponding to a point x by $\boldsymbol{x}$ or $\overrightarrow{Ox}$, the latter being the preferred notation when one has to specify the origin explicitly.

To start with, we consider the non-periodic solution to (8), (9), (10) and (11) in $\mathbb{R}^3$ with an asymptotic condition given by

$$\chi_i^{pq}(x) \to 0 \quad (|\boldsymbol{x}| \to \infty)$$

instead of the periodic condition. Then the solution χ_i^{pq} has an integral representation given by

$$\chi_i^{pq}(x) = \int_{\partial\sigma} \Gamma_{is}(\boldsymbol{x} - \boldsymbol{y}) t_s^{pq}(y) ds_y \quad \text{in } \Omega, \tag{14}$$

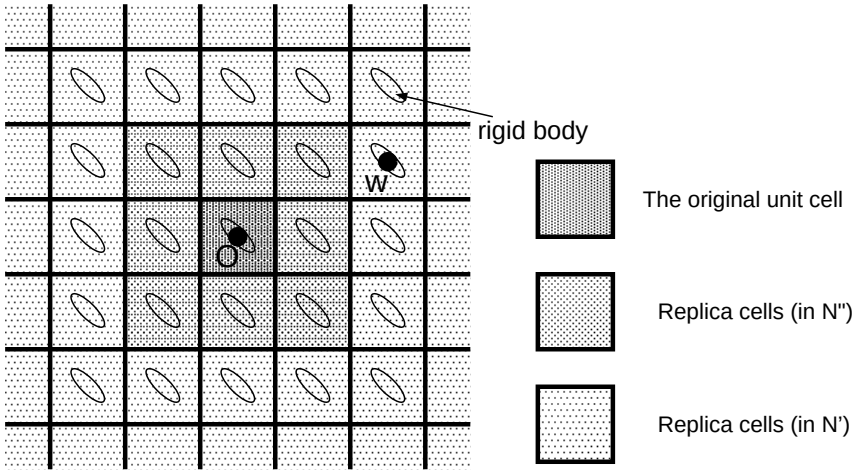

Figure 2: Original unit cell and replicas

where $\Gamma_{ij}(\boldsymbol{x}-\boldsymbol{y})$ is the fundamental solution of the equation of the elastostatics expressed as

$$\Gamma_{ij}(\boldsymbol{x}-\boldsymbol{y}) = \frac{1}{8\pi\mu}\left(\delta_{ij}\frac{\partial}{\partial x_l}\frac{\partial}{\partial x_l} - \frac{\lambda+\mu}{\lambda+2\mu}\frac{\partial}{\partial x_i}\frac{\partial}{\partial x_j}\right)|\boldsymbol{x}-\boldsymbol{y}|.$$

Letting x approach $\partial\sigma_{(l)}$, we obtain the boundary integral equation given by:

$$-\delta_{pi}x_q + c^{pq}_{(l)i} + e_{ijk}w^{pq}_{(l)j}x_k = \int_{\partial\sigma}\Gamma_{is}(\boldsymbol{x}-\boldsymbol{y})t^{pq}_s(y)ds_y\ . \tag{15}$$

We shall now periodise the RHS of (15). At the first sight it might appear that a periodic solution is obtained easily as one introduces boundary elements on the exterior boundary of the original unit cell. But this is not true. Indeed, this method is not suitable in the analysis of complicated models because it requires additional DOFs on the exterior boundary. In addition, the coefficient matrix thus obtained is ill-conditioned, as we shall see. We shall therefore use a different approach.

The method we propose in this paper is based on an idea related to the renormalisation approach used in Greengard and Rokhlin[3]. Indeed, we shall put infinite number of replicas of the unit cell around the original unit cell as shown in Figure 2.

Apparently it seems sufficient to take the sum of the RHS of (14) in the following manner:

$$\begin{aligned}&\int_{\partial\sigma}\gamma'_{is}(\boldsymbol{x}-\boldsymbol{y})t^{pq}_s(y)ds_y,\\ &\gamma'_{ij}(\boldsymbol{x}-\boldsymbol{y}) = \sum_w \Gamma_{is}(\boldsymbol{x}-\boldsymbol{y}-\boldsymbol{w}),\end{aligned} \tag{16}$$

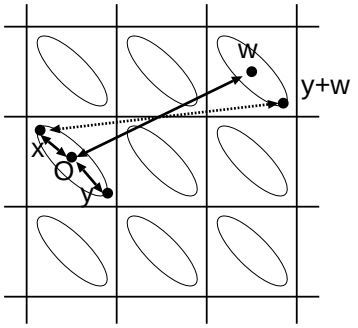

Figure 3: Points x, y, w and O

where w is the centre of replicas and x and y are on $\partial\sigma$ in the original unit cell (see Figures 2 and 3). But the summation thus obtained is divergent since the summand is $O(|\boldsymbol{w}|^{-1})$, hence one cannot compute the sum without mathematical ambiguity. In Greengard and Rokhlin[3] these authors use a physical argument to replace the divergent series by finite numbers in the Laplace case in 2D. In the present paper, however, we shall use a more formal approach where no divergent series appear.

To deal with this issue of summation, we recall that the multipole expansion of the fundamental solution of elasticity is given by [10]

$$\begin{aligned}
\Gamma_{ij}\left(\boldsymbol{x}-\boldsymbol{y}-\boldsymbol{w}\right) =& \frac{1}{8\pi\mu}\left\{\sum_{n=0}^{\infty}\sum_{m=-n}^{n}\overline{S_{n,m}(\overrightarrow{Ow})}F^R_{ij,n,m}(\overrightarrow{yx})\right. \\
&\left.+\sum_{n=1}^{\infty}\sum_{m=-n}^{n}\overline{S_{n,m}(\overrightarrow{Ow})}(\overrightarrow{Ow})_j G^R_{i,n,m}(\overrightarrow{yx})\right\} \\
=& \frac{1}{8\pi\mu}\sum_{n=0}^{\infty}\sum_{m=-n}^{n} \\
&\left\{F^R_{ij,n,m}(\overrightarrow{Ox})\sum_{n'=0}^{\infty}\sum_{m'=-n'}^{n'}(-1)^{n'}\overline{S_{n+n',m+m'}(\overrightarrow{Ow})}\,R_{n',m'}(\overrightarrow{Oy})\right. \\
&+G^R_{i,n,m}(\overrightarrow{Ox})\sum_{n'=0}^{\infty}\sum_{m'=-n'}^{n'}(-1)^{n'}\overline{S_{n+n',m+m'}(\overrightarrow{Ow})} \\
&\left.\times\left((\overrightarrow{Oy})_j R_{n',m'}(\overrightarrow{Oy})+(\overrightarrow{Ow})_j R_{n',m'}(\overrightarrow{Oy})\right)\right\} \qquad (17)
\end{aligned}$$

where

$$F^R_{ij,n,m}(\overrightarrow{Ox}) = \frac{\lambda+3\mu}{\lambda+2\mu}\delta_{ij}R_{n,m}(\overrightarrow{Ox}) - \frac{\lambda+\mu}{\lambda+2\mu}(\overrightarrow{Ox})_j\frac{\partial}{\partial x_i}R_{n,m}(\overrightarrow{Ox}),$$
$$G^R_{i,n,m}(\overrightarrow{Ox}) = \frac{\lambda+\mu}{\lambda+2\mu}\frac{\partial}{\partial x_i}R_{n,m}(\overrightarrow{Ox}),$$

$S_{n,m}$ and $R_{n,m}$ are defined as

$$S_{n,m}(\overrightarrow{Ox}) = (n-m)!P^m_n(\cos\theta)e^{im\phi}\frac{1}{r^{n+1}},$$
$$R_{n,m}(\overrightarrow{Ox}) = \frac{1}{(n+m)!}P^m_n(\cos\theta)e^{im\phi}r^n \ ,$$

(r,θ,ϕ) are the spherical coordinates of the point x, and P^m_n stands for the associated Legendre function, respectively. In order to make the summation in (16) convergent, we subtract first few terms in the multipole series from (17) in the following manner:

$$\begin{aligned}\gamma_{ij}(\boldsymbol{x}-\boldsymbol{y}) = &\Gamma_{ij}(\boldsymbol{x}-\boldsymbol{y})\\ &+\sum_{w\in N''}\Gamma_{ij}(\boldsymbol{x}-\boldsymbol{y}-\boldsymbol{w})\\ &+\sum_{w\in N'}\{\Gamma_{ij}(\boldsymbol{x}-\boldsymbol{y}-\boldsymbol{w}) - D_{ij}(\boldsymbol{x}-\boldsymbol{y},w)\}, \end{aligned} \tag{18}$$

where N'' and N' are defined as

$$\begin{aligned} N'' &= \{(x,y,z)=(l,m,n)| \quad l,m,n\in\{-1,0,1\},\ (x,y,z)\neq(0,0,0)\},\\ N' &= N\setminus N'',\\ N &= \{(x,y,z)=(l,m,n)| \quad l,m,n\in\mathbb{Z},\ (x,y,z)\neq(0,0,0)\},\end{aligned}$$

and $D_{ij}(\boldsymbol{x}-\boldsymbol{y},w)$ is defined by

$$\begin{aligned}D_{ij}(\boldsymbol{x}-\boldsymbol{y},w) = \frac{1}{8\pi\mu}\Bigg\{&\sum_{n=0}^{2}\sum_{m=-n}^{n}\overline{S_{n,m}(\overrightarrow{Ow})}F^R_{ij,n,m}(\overrightarrow{yx})\\ &+\sum_{n=1}^{3}\sum_{m=-n}^{n}\overline{S_{n,m}(\overrightarrow{Ow})}(\overrightarrow{Ow})_jG^R_{i,n,m}(\overrightarrow{yx})\Bigg\}\ .\end{aligned}$$

The series in (18) is absolutely convergent since the function D_{ij} removes terms of the minus 1st, 2nd and 3rd powers of $|\overrightarrow{Ow}|$ from γ_{ij}. Obviously, γ_{ij} is a solution of elastostatics with respect to x because both Γ_{ij} and D_{ij} are. We also notice that D_{ij} is quadratic with respect to $\boldsymbol{r}(=\boldsymbol{x}-\boldsymbol{y})$. Therefore, the 2nd derivatives of γ_{ij} are periodic, from which we conclude the following:

$$\gamma_{ij}(\boldsymbol{r}+\boldsymbol{w}_t) = \gamma_{ij}(\boldsymbol{r}) + \eta^{ij,t}_p r_p + \kappa^{ij,t},$$

where w_t is the unit vector directed to t-th coordinate axis and $\eta_p^{ij,t}$ and $\kappa^{ij,t}$ are constants.

The numbers $\eta_p^{ij,t}$ are obtained as follows:

$$\begin{aligned}\eta_p^{ij,t} &= \frac{\partial \gamma_{ij}}{\partial r_p}(\boldsymbol{r}^{t+}) - \frac{\partial \gamma_{ij}}{\partial r_p}(\boldsymbol{r}^{t-}) \\ &= \lim_{R\to\infty}\left[\sum_{w\in \mathrm{Sym}(R)}\left\{\frac{\partial \Gamma_{ij}}{\partial r_p}(\boldsymbol{r}^{t+}-\boldsymbol{w}) - \frac{\partial \Gamma_{ij}}{\partial r_p}(\boldsymbol{r}^{t-}-\boldsymbol{w})\right\}\right. \\ &\qquad \left. + \sum_{w\in N'(R)}\left\{\frac{\partial D_{ij}}{\partial r_p}(\boldsymbol{r}^{t+},w) - \frac{\partial D_{ij}}{\partial r_p}(\boldsymbol{r}^{t-},w)\right\}\right],\end{aligned}$$

where $(\boldsymbol{r}^{t\pm})_i = \pm\frac{1}{2}\delta_{ti}$, and $\mathrm{Sym}(R)$ and $N'(R)$ are the sets defined as

$$\begin{aligned}\mathrm{Sym}(R) &= \{(x,y,z)=(l,m,n)| \quad l,m,n\in\mathbb{Z},\ l,m,n\le R\} \\ N'(R) &= \mathrm{Sym}(R)\setminus N'' \ ,\end{aligned}$$

respectively. With a lengthy but straight-forward calculation, one shows that $\eta_p^{ij,t}$ are expressed as

$$\begin{aligned}\eta_i^{ii,i} &= \frac{1}{8\pi\mu}\left(-2\alpha + \frac{\lambda+\mu}{\lambda+2\mu}\zeta\right) && (i=1,2,3),\\ \eta_j^{ii,j} &= \frac{1}{8\pi\mu}\left(-\frac{\lambda+3\mu}{\lambda+2\mu}\alpha - \frac{\lambda+\mu}{2(\lambda+2\mu)}\zeta\right) && (i,j\in\{1,2,3\},\ i\neq j),\\ \eta_j^{ij,i} = \eta_i^{ij,j} &= \frac{1}{8\pi\mu}\left(\frac{\lambda+\mu}{\lambda+2\mu}\alpha - \frac{\lambda+\mu}{2(\lambda+2\mu)}\zeta\right) && (i,j\in\{1,2,3\},\ i\neq j),\end{aligned}$$

where

$$\begin{aligned}\alpha &= 2\lim_{R\to\infty}\sum_{w\in\mathrm{Sym}(R)}\frac{\frac{1}{2}-w_1}{|\boldsymbol{r}^{1+}-\boldsymbol{w}|^3} \sim 4.1888\\ \zeta &= \lim_{R\to\infty}\left[12\sum_{w\in\mathrm{Sym}(R)}\frac{w_2^2(\frac{1}{2}-w_1)}{|\boldsymbol{r}^{1+}-\boldsymbol{w}|^5} - \sum_{w\in N'(R)}\left(\frac{15w_3^4}{|w|^7}-\frac{9w_3^2}{|w|^5}\right)\right] \sim 3.5131\end{aligned}$$

Notice that α and ζ are given in convergent series. Indeed, one has

$$\begin{aligned}\alpha &= 2\lim_{R\to\infty}\sum_{w\in\mathrm{Sym}(R)}\left(-\frac{w_1}{r^3}+\frac{(w_2^2-w_1^2)+(w_3^2-w_1^2)}{2r^5}+O(r^{-4})\right)\\ &= 2\lim_{R\to\infty}\sum_{w\in\mathrm{Sym}(R)}O(r^{-4})\end{aligned}$$

and a similar result for ζ, where $r=\sqrt{w_1^2+w_2^2+w_3^2}$.

We now use γ_{ij} to construct a Y-periodic solution of elastostatics in the following form:

$$P_i(x) = \int_{\partial\sigma} \left[\gamma_{ij}(\boldsymbol{x}-\boldsymbol{y}) + x_q \eta_p^{ij,q} y_p\right] t_j ds_y, \tag{19}$$

where (10) has been used. With this result, the boundary integral equation for periodic problems reduces to

$$-\delta_{pi}x_q + c_{(l)i}^{pq} + e_{ijk} w_{(l)j}^{pq} x_k = \int_{\partial\sigma} \left[\gamma_{ij}(\boldsymbol{x}-\boldsymbol{y}) + x_s \eta_r^{ij,s} y_r\right] t_j^{pq}(y) ds_y \ . \tag{20}$$

This equation is augmented with equilibrium conditions given by

$$\int_{\partial\sigma_{(l)}} t_i^{pq} ds = 0, \quad \int_{\partial\sigma_{(l)}} e_{ijk} t_j^{pq} y_k ds = 0$$

for each of $\sigma_{(l)}$. The solution t_i^{pq}, $c_{(l)i}^{pq}$ and $w_{(l)j}^{pq}$ of the system given above is easily seen to be unique, since the aditional arbitrariness of $c_{(l)i}^{pq}$ has already been resolved in the process of sellecting γ_{ij}.

3 Algorithm

In this section we shall briefly describe the algorithm used in the present investigation, which basically follows the approach used in Greengard and Rokhlin[3]. Namely, we take the unit cell to be the level 0 cell, and apply the ordinary FMM algorithm (See Nishimura[1], Liu et al.[2] and Yoshida et al.[10] for the datail of the ordinary FMM for elastostatics in 3D) to the terms of the integral in (19) which come from the first and second terms in the expression (18) for γ_{ij}. The contributions to the integral in (19) from the third term in (18) and the linear term (i.e. $x_q \eta_p^{ij,q} y_p$) are evaluated in the form of the coefficients of the local expansion of the level 0.

The algorithm goes as follows:

1. upward pass
   From the lowest level to the level 0, we calculate multipole moments at the centre of every cell. In elasticity, the multipole moments $M_{j,n,m}^1(O_c)$ and $M_{n,m}^2(O_c)$ of a cell C centred at O_c are defined by [2]

$$M_{j,n,m}^1(O_c) = \int_{\partial\sigma \bigcap C} R_{n,m}(\overrightarrow{O_c y}) t_j(y) dS_y,$$

$$M_{n,m}^2(O_c) = \int_{\partial\sigma \bigcap C} (\overrightarrow{O_c y})_j R_{n,m}(\overrightarrow{O_c y}) t_j(y) dS_y \ .$$

   The required manipulations for this process are exactly the same as those in the ordinary FMM for elastostatics except that one goes up to the level 0 cell. After this process the multipole moments of level 0 denoted by $M_{j,n,m}^1(O)$ and $M_{n,m}^2(O)$ are obtained.

2. lattice sum

At the level 0, we calculate the effects from the replicas of the unit cell whose centres are in N' and the effect of the linear term (the second term of the RHS) in (19), and write the sum of these contributions in the following form

$$\frac{1}{8\pi\mu}\sum_{n=0}^{\infty}\sum_{m=-n}^{n}\left\{F^R_{ij,n,m}(\overrightarrow{Ox})L^1_{j,n,m}(O)+G^R_{i,n,m}(\overrightarrow{Ox})L^2_{n,m}(O)\right\}\ ,$$

where $L^1_{j,n,m}(O)$ and $L^2_{n,m}(O)$ are the coefficients of the local expansion of the level 0.

To this end, we use the following formula to convert the level 0 multipole moments $M^{\cdot}_{\cdot}(O)$ into the level 0 coefficients of local expansion $L^{\cdot}_{\cdot}(O)$ centerd at O:

$$\begin{aligned}
L^1_{j,n,m}(O) &= \sum_{w\in N'}\sum_{n'=\max(0,3-n)}^{\infty}\sum_{m'=-n'}^{n'}(-1)^{n'}\overline{S_{n+n',m+m'}(\overrightarrow{Ow})}M^1_{j,n',m'}(O),\\
&\quad+\delta_{n1}L^{\rm lin}_{j,m}\\
L^2_{n,m}(O) &= \sum_{w\in N'}\left(\sum_{n'=\max(0,3-n)}^{\infty}(-1)^{n'}\sum_{m'=-n'}^{n'}\overline{S_{n+n',m+m'}(\overrightarrow{Ow})}M^2_{n',m'}(O)\right.\\
&\quad\left.+\sum_{n'=\max(0,4-n)}^{\infty}(-1)^{n'}\sum_{m'=-n'}^{n'}\overline{S_{n+n',m+m'}(\overrightarrow{Ow})}(\overrightarrow{Ow})_jM^1_{j,n',m'}(O)\right).
\end{aligned}$$

In the above formulae the term $L^{\rm lin}_{i,j}$ includes the effect of the linear terms while other terms gives the contributions from the replicas in N'. The expression for $L^{\rm lin}_{i,j}$ is given in terms of the level 0 multipole moments, $\eta^{ij,k}_l$ and Lamé's constants as

$$L^{\rm lin}_{i,1}=L'_{i,1}-iL'_{i,2},\quad L^{\rm lin}_{i,-1}=-\left(L'_{i,1}+iL'_{i,2}\right),\quad L^{\rm lin}_{i,0}=L'_{i,3},\qquad(21)$$

where the numbers $L'_{i,j}$ are given by

$$\begin{aligned}
L'_{i,i}&=C'\left[M'_{i,i}(\eta^{11,1}_1-\eta^{12,1}_2)+\left(\sum_{j=1}^{3}M'_{j,j}\right)\eta^{12,1}_2\right]\quad(i=1,2,3)\\
L'_{i,j}&=C'M'_{i,j}(\eta^{11,2}_2+\eta^{12,1}_2)\quad(i,j\in\{1,2,3\},\ i\neq j),
\end{aligned}\qquad(22)$$

with

$$C'=\frac{\lambda+2\mu}{2\mu},\qquad(23)$$

$$\begin{aligned}
&M'_{1,i}=M^1_{1,1,i}(O)-M^1_{-1,1,i}(O),\quad M'_{2,i}=\frac{1}{i}\left(M^1_{1,1,i}(O)+M^1_{-1,1,i}(O)\right),\\
&M'_{3,i}=M^1_{0,1,i}(O).
\end{aligned}$$

Notice that $M'_{i,j}$ is symmetric with respect to i and j when $\sigma_{(l)}$ does not intersect with ∂Y. However, this is not the case when $\sigma_{(l)}$ crosses ∂Y. See **Appendix** for required modifications to the formulae (22) and (23) in this case.

3. downward pass
   From the level 0 to the bottom cell, we calculate coefficients of local expansion at the centre of every cell. The interaction lists of cells contain cells whose centres are in N''' defined as

$$N''' = \{(l,m,n)| \quad l,m,n \in \{-1,0,1\}\} \ .$$

In the numerical implementation we need the following lattice sums in the step 2:

$$\sum_{w \in N'} \overline{S_{n,m}(\overrightarrow{Ow})} \quad (n \geq 3), \tag{24}$$

$$\sum_{w \in N'} \overline{S_{n,m}(\overrightarrow{Ow})}(\overrightarrow{Ow})_i \quad (n \geq 4) \tag{25}$$

which can be precomputed easily since all of these sums are absolutely convergent. Notice that the sum in (24) is nonzero only when n is even and m is a multiple of 4. Also, the sum in (25) is nonzero only when n is odd and m is odd when $i = 1, 2$ and m is a multiple of 4 when $i = 3$.

4 Numerical Results

4.1 Tests of accuracy

In order to examine the accuracy of proposed method for periodic problems, we carry out numerical experiments for the following two cases:

Case 1 present method:

Case 2 ordinary method:

Namely, we use conventional boundary integral equation method putting boundary elements on the boundary of the original unit cell in order to impose the periodic boundary condition.

We consider a rigid sphere with the radius of 0.4 located at the centre of the unit cell, which is a cube having the side length of 1. The frame in Figure 4 represents the unit cell. The sphere is divided into 980 boundary elements, and the boundary of the unit cell is divided into 1728 elements in Case 2. The matrix outside of the rigid sphere is an elastic body with $\lambda = \mu = 1$. The governing equation is (8), and boundary conditions are given by (9), (10), (11) and (12). Two cases with $(p,q) = (1,1)$ and $(p,q) = (1,2)$ are considered. The solver of

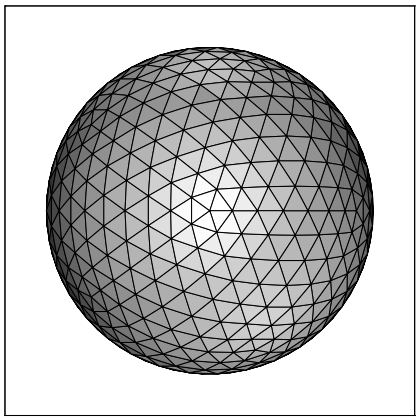

Figure 4: Boundary elements on the sphere

the linear equation is GMRES with no restart and the iteration is terminated when the relative error is less than 10^{-5}. The preconditioner for GMRES is chosen to be the one corresponding to the ordinary boundary element matrix of one rigid sphere in an infinite domain.

Table 1 compares the numerical solutions for Cases 1 and 2, where the difference of the two solutions for the three components of the traction on the sphere is indicated. The error is defined as

$$\frac{\sum_n \sqrt{(t_i^1(x_n) - t_i^2(x_n))^2}}{\sum_n \sqrt{(t_i^1(x_n))^2}},$$

where the superscript I ($I = 1, 2$) stands for the Case I results. Table 1 clearly shows the validity of the proposed method. Although the error of t_3 for $(p, q) = (1, 2)$ is larger than those of other cases, it is just because the norm of t_3 is one order smaller than others.

Also shown in Table 1 is the number of iterations of GMRES in each case. As is seen, there is a significant difference in the number of iterations between Cases 1 and 2. This indicates better conditioning of the matrix obtained with the proposed method than that of the ordinary approach with the discretised exterior boundary. This improved conditioning is considered to be an advantage of the proposed method.

4.2 Application to the homogenisation method

In this section we calculate macroscopic elastic constants of composites with rigid inclusions using the homogenisation method (see (13)). Two types of microscopic structures are examined. Namely, we consider composites with rigid spherical inclusions and those with fibres.

Table 1: Comparison of numerical solutions

error	$(p,q)=(1,1)$	$(p,q)=(1,2)$
t_1	2.95×10^{-3}	3.45×10^{-3}
t_2	5.16×10^{-3}	3.42×10^{-3}
t_3	5.42×10^{-3}	3.17×10^{-2}
number of iteration (Case 1)	6	4
number of iteration (Case 2)	151	165

As a matter of fact, it is sufficient to consider 6 cases out of the 9 combinations of (p,q) in (20) in order to obtain all the components of the macroscopic elastic constants. In the present investigation, however, we solved all these 9 cases to check the required symmetry of the solutions.

4.2.1 Spherical inclusion

We consider a rigid spherical inclusion having the radius of $r = 0.16$, 0.2, 0.25, 0.27, 0.3, 0.4 located at the centre of the unit cell. We are interested in estimating the macroscopic elastic constants of the composite having this unit cell as the microstructure. The Lamé constants of the matrix are chosen to be $\lambda_0 = 0.576923$ and $\mu_0 = 0.384615$ so that Young's modulus and Poisson's ratio are given by $E_0 = 1.0$ and $\nu_0 = 0.3$, respectively.

As a matter of fact, it is possible to estimate the macroscopic elastic constants of such composites with the help of micromechanics[11]. Indeed, the well-known method of Eshelby tells that the macroscopic shear and bulk moduli $\overline{\mu}$ and $\overline{K}$ of this material are estimated as

$$\frac{\overline{\mu}}{\mu_0} = \frac{1}{1-\frac{\phi}{2S_{1212}}}, \quad \frac{\overline{K}}{K_0} = \frac{1}{1-\frac{\phi}{\frac{1}{3}S_{iijj}}}$$

in the limit as the stiffness of the sphere tends to infinity, where

$$S_{1212} = \frac{4-5\nu}{15(1-\nu)}, \quad S_{iijj} = \frac{1+\nu}{1-\nu},$$

and ϕ is the volume fraction of the fibres in the composite. Also, the use of the self-consistent method gives

$$\overline{\mu} = \mu_0 + \frac{\phi\overline{\mu}}{2S_{1212}}, \quad \overline{K} = K_0 + \frac{\phi\overline{K}}{\frac{1}{3}S_{iijj}},$$

where

$$S_{1212} = \frac{4-5\overline{\nu}}{15(1-\overline{\nu})}, \quad S_{iijj} = \frac{1+\overline{\nu}}{1-\overline{\nu}}, \quad \overline{\nu} = \frac{3\overline{K}-2\overline{\mu}}{2(\overline{\mu}+3\overline{K})}\ .$$

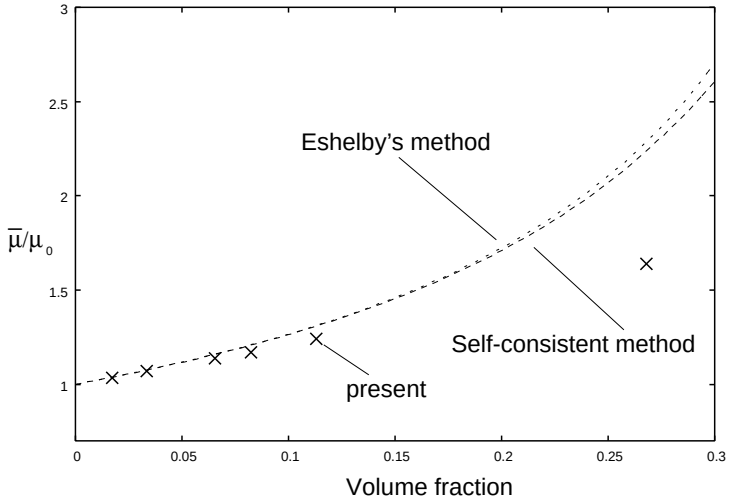

Figure 5: Macroscopic shear modulus versus volume fraction of the rigid sphere

We now compare the macroscopic elastic constants obtained with the proposed approach with those obtained with Eshelby's method and the self-consistent method. Figure 5 gives the estimated macroscopic shear modulus $\overline{\mu}$, and Figure 6 shows the similar estimate for the macroscopic bulk modulus $\overline{K}$. Good agreement between the results obtained with these methods is observed for lower values of the volume fractions, while the results of the present approach deviate from the micromechanical estimates for higher volume fractions. This is to be expected because both Eshelby's method and self-consistent method do not rigorously take the interaction between rigid spheres into account.

4.2.2 Short-fibre composites

An array of $1 \times m \times m$ short fibres with the length of $l = 0.8$ and the radius of $r = 0.1$ are studied for $m = 1, 2, 3, 4$ (See Figure 7). The fibres are directed into the x_1 direction and the arrays of fibres are placed evenly inside the unit cell. However, positions of the fibres in the x_1 direction are shifted for every other fibre by the distance which is equal to one half of the side length of the unit cell. When a fibre crosses the boundary of the unit cell, the part of the fibre outside the unit cell is moved to the opposite side of the unit cell (See Figure 8). The estimated moduli of elasticity are compared with those obtained with the Halpin-Tsai equation[2], which is a well-accepted empirical expression given by

$$\frac{\overline{E}}{E_0} = \frac{1 + 2\xi\phi}{1 - \phi},$$

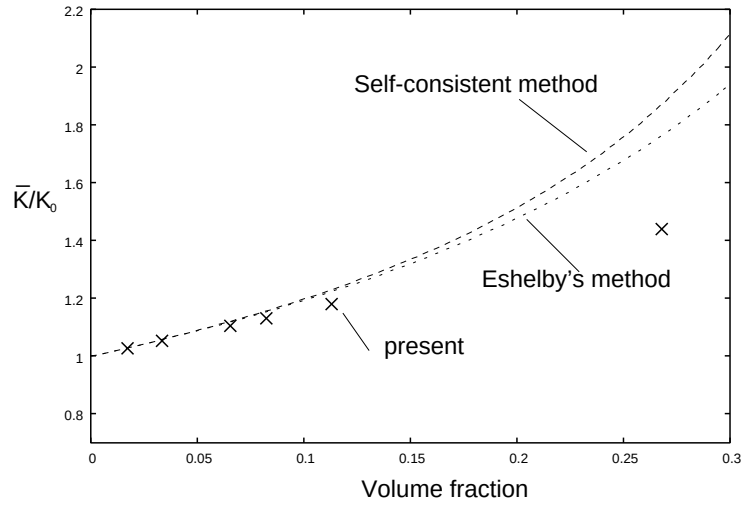

Figure 6: Macroscopic bulk modulus versus volume fraction of the rigid sphere

where $\overline{E}$ and E_0 are Young's modulus of the composite and matrix, $\xi = l/2r$ is the fibre aspect ratio and ϕ is the volume fraction of the fibres in the composite, respectively. The Lamé constants of the matrix are chosen to be $\lambda_0 = 5.42857$ and $\mu_0 = 1.35714$ so that Young's modulus and Poisson's ratio are $E_0 = 3.8$ and $\nu_0 = 0.4$, respectively. The preconditioner for GMRES is chosen to be the one corresponding to the ordinary boundary element matrix of one rigid fibre in an infinite domain.

Figure 9 shows the estimated macroscopic Young's modulus $\overline{E}$ and those obtained with the Halpin-Tsai equation. Good agreement is observed.

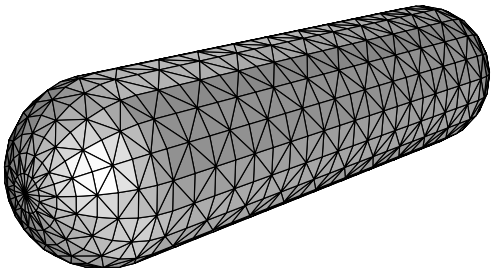

Figure 7: Short fibre (with 1400 elements)

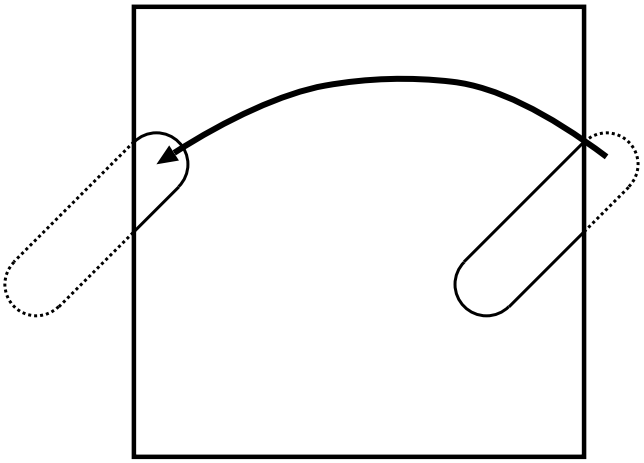

Figure 8: A fibre crossing the boundary of the unit cell

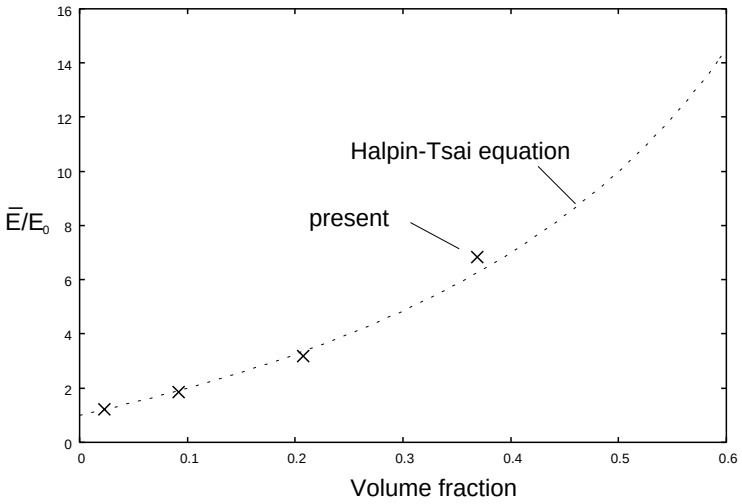

Figure 9: Macroscopic Young's modulus versus volume fraction of the fibres

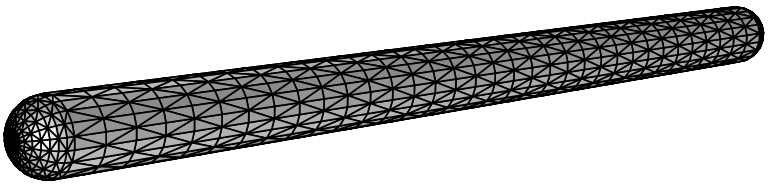

Figure 10: Long fibre

4.2.3 Long-fibre composites

Finally, we consider a composite including many long fibres. As shown in Figure 10, the model for the inclusion is a slender one whose length is 0.8 and the radius is 0.025. Arrays of $1 \times m \times m$ fibres are placed evenly inside the unit cell. The cases studied include $m = 1, 2, 3, 4, 5, 6, 8$. As Figure 11 shows, the fibres are aligned in the x_1 direction and the positions of the fibres in the x_1 direction are shifted for every other fibre by a distance which is equal to one half of the side length of the unit cell. The Lamé constants of the matrix are the same as the short fibre case. Each fibre surface is subdivided into 1960 boundary elements. The preconditioner for GMRES is chosen to be the one corresponding to the ordinary boundary element matrix of one rigid fibre in an infinite domain.

Figure 12 shows the estimated macroscopic Young's moduli $\overline{E}$, and Table 2 presents the components of the estimated macroscopic elastic constants C_{ijkl} for $m = 8$.

All the numerical examples in this subsection were obtained with FUJITSU PRIMEPOWER HPC2500 of Academic Center for Computing and Media Studies of Kyoto University, which has 128 CPUs (SPARC64V, 2.08GHz) and 512GB of shared memory. 32 CPUs were used for the present analysis. The computation for the largest problem with 376,704 DOF ($m = 8$) took 5214 seconds for the total of 9 runs corresponding to the 9 combinations of (p, q) in (20).

5 Conclusions

In this paper, we developed an FMM for periodic elastostatic problems in 3D. The basic idea of the method is similar to that proposed by Greengard & Rokhlin in that both methods periodise the solution by using replica cells. The most significant difference between these approaches, however, is the way of taking the lattice sums of the fundamental solution. Central to the development of our method is the subtraction of first few terms in the multipole expansions of the fundamental solution from the kernel function. With this operation both divergent series in the formulation and mathematical ambiguity are removed. Our method uses no physical arguments or 'renormalisation' because no divergent

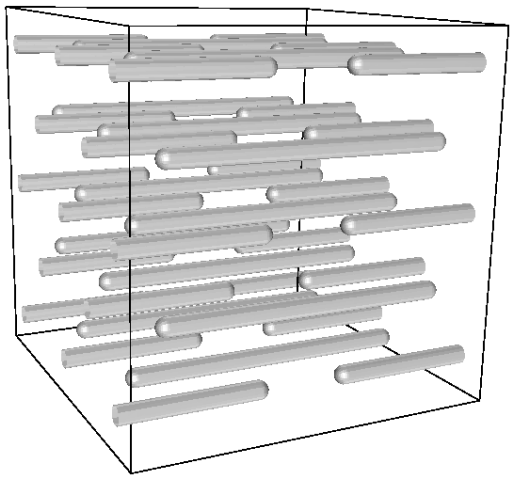

Figure 11: Alignment of long fibres (m=5)

Table 2: Macroscopic elastic coefficients C_{ijkl} ($m = 8$, 376704DOF)

$ijkl$	without fibre	with fibre
1111	8.14	36.2
2222	8.14	9.30
3333	8.14	9.30
1122	5.43	6.04
1133	5.43	6.04
2233	5.43	6.03
1212	1.36	1.66
1313	1.36	1.66
2323	1.36	1.59

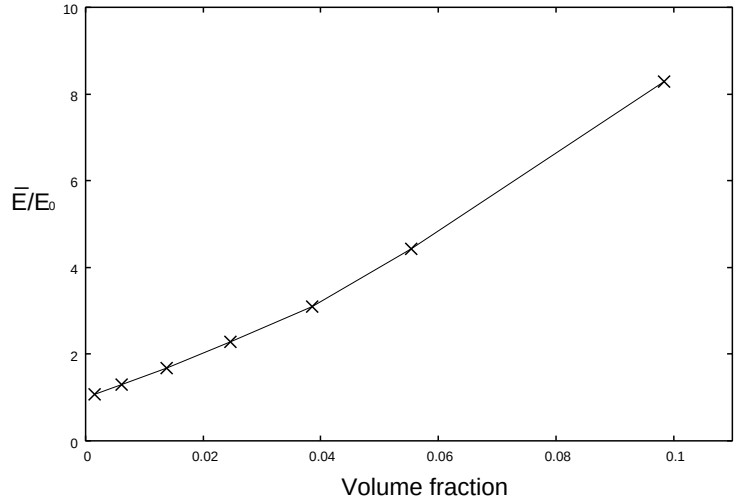

Figure 12: Macroscopic Young's modulus versus volume fraction of the fibres

series occurs. We validated the proposed method by carrying out numerical experiments,

We then applied the priodic FMM to the homogenisation theory. Homogenisation methods require solutions of periodic boundary value problems in obtaining macroscopic elastic coefficients C'_{ijkl} of the target model. As target models, we considered composites which consist of elastic matrix and many rigid inclusions. Numerical solutions were compared to those obtained with Eshelby's method and self-consistent method or the Halpin-Tsai equation, and in each of these cases good agreement was observed.

6 Acknowledgment

This research was partially supported by the Ministry of Education, Science, Sports and Culture, Grant-in-Aid for JSPS Fellows, 17·2202. The authors also thank Prof. Y.J. Liu of University of Cincinnati for directing our attention to CNT based composite problems and for providing meshes for fibres.

References

[1] N. Nishimura: Fast multipole accelerated boundary integral equation methods, *Applied Mechanics Reviews*, **55** (2002), pp.299–324.

[2] Y. J. Liu, N. Nishimura, and Y. Otani: Large-scale modeling of carbon-nanotube composites by a fast multipole boundary element method, *Computational Materials Science*, in press.

[3] L. Greengard and V. Rokhlin: A fast algorithm for particle simulations, *Journal of Computational Physics*, **73**(1987), pp.325–348.

[4] L. Greengard and J. Helsing: On the numerical evaluation of elastostatic fields in locally isotropic two-dimensional composites, *Journal of the Mechanics and Physics of Solids*, **46**(1998), pp.1441–1462.

[5] G. J. Rodin and J. R. Overfelt: Periodic conduction problems: the fast multipole method and convergence of integral equations and lattice sums, *Proceedings of the Royal Society of London, Series A*, **460**(2004), pp.2883–2902.

[6] A. S. Sangani and G. Mo: An $O(N)$ algorithm for Stokes and Laplace interactions of particles, *Physics of Fluids*, **8**(1996), pp.1990–2010.

[7] A. Z. Zinchenko and R. H. Davis: An efficient algorithm for hydrodynamical interaction of many deformable drops, *Journal of Computational Physics*, **157**(2000), pp.539–587.

[8] L. Greengard, M. C. Kropinski: Integral equation methods for Stokes flow in doubly-periodic domains, *Journal of Engineering Mathematics*, **48**(2004), pp.157–170.

[9] J.L. Lions: Remarks on some asymptotic problems in composite and in perforated materials, *Variational Methods in the Mechanics of Solids (Ed. S. Nemat-Nasser)*, Pergamon, (1980), pp.3–20.

[10] K. Yoshida, N. Nishimura, and S. Kobayashi: Application of fast multipole Galerkin boundary integral equation method to elastostatic crack problems in 3D, *International Journal for Numerical Methods in Engineering*, **50**(2001), pp.525–547.

[11] T. Mura: *Micromechanics of Defects in Solids*, Martinus Nijhoff Publishers, Amsterdam, 1982.

Appendix

Some of the formulae presented in the main body of this paper have to be modified when the inclusion $\sigma_{(l)}$ crosses ∂Y. Suppose, for example, that $\sigma_{(l)}$ crosses ∂Y at $y_t = 1/2$ for a certain t ($t = 1, 2, 3$). The part of the rigid body which extends beyond $y_t = 1/2$ is then moved to the other side of Y. Namely, the set $\sigma_{(l)}$ is divided into two parts; one near $y_t = 1/2$ and the other near $y_t = -1/2$. We then have to modify (11) and (13) as

$$\int_{\partial\sigma_{(l)}} e_{irs} C_{rjkl} y_s \chi^{pq}_{k,l} n_j ds_y + \int_{\partial\sigma_{(l)} \bigcap \sigma^+_{(l)}} e_{irs} C_{rjkl} \delta_{ts} \chi^{pq}_{k,l} n_j ds_y = 0,$$

$$C'_{ijkl} = C_{ijkl} - \frac{1}{|Y|}\int_{\partial\sigma} t_i^{kl} y_j ds - \frac{1}{|Y|}\int_{\partial\sigma \bigcap \sigma^+} t_i^{kl}\delta_{jt} ds$$

respectively where $\sigma^+_{(l)}$ is the part of $\sigma_{(l)}$ moved to the opposite side of the unit cell (See Figure 8) and $\sigma^+ = \bigcup_l \sigma^+_{(l)}$. Similarly, we have to modify (15) as

$$-\delta_{pi}(x_q + \delta_{qt}) + c^{pq}_{(l)i} + e_{ijk} w^{pq}_{(l)j}(x_k + \delta_{kt}) = \int_{\partial\sigma} \Gamma_{is}(\boldsymbol{x} - \boldsymbol{y}) t_s^{pq}(y) ds_y$$

when $x \in \partial\sigma^+$. Also, (23) is now replaced by

$$L'_{i,j} = M'_{i,j}(\eta_2^{11,2} B' + \eta_2^{12,1} A') + M'_{j,i}(\eta_2^{11,2} A' + \eta_2^{12,1} B') \quad (i, j \in \{1,2,3\},\ i \neq j),$$

where

$$A' = \frac{\lambda + 3\mu}{4\mu}, \quad B' = \frac{\lambda + \mu}{4\mu}.$$

Notice that $M'_{i,j}$ is no longer symmetric.